Available online at www.sciencedirect.com
ScienceDirect
Journal of Molecular Catalysis A: Chemical 270 (2007) 295–301
JOURNAL OF MOLECULAR CATALYSIS A: CHEMICAL
www.elsevier.com/locate/molcata

Strong templating effect of TEAOH in the hydrothermal genesis of the $AlPO_4$-5 molecular sieve: Experimental and computational investigations

Mohamed Elanany [a,b], Bao-Lian Su [b,*], Daniel P. Vercauteren [a,**]

[a] *Laboratoire de Physico-Chimie Informatique, University of Namur, 61 Rue de Bruxelles, Namur B-5000, Belgium*
[b] *Laboratorie de Chimie des Matériaux Inorganiques, University of Namur, 61 Rue de Bruxelles, Namur B-5000, Belgium*

Received 4 December 2006; received in revised form 6 February 2007; accepted 12 February 2007
Available online 20 February 2007

Abstract

The hydrothermal genesis of $AlPO_4$-5, in the presence of four different organic templates, viz., methyldicyclohexylamine (MCHA), triethylamine (TEA), tripropylamine (TPA), and tetraethylammonium hydroxide (TEAOH), has been monitored by XRD. It is shown that TEAOH has the best templating ability to the formation of $AlPO_4$-5 structure under the different synthesis conditions considered in this study. Density functional calculations on periodic models of $AlPO_4$-5 indicate the strongest nonbonding interaction energy between the template and the framework in the case of TEAOH. Therefore, a new approach correlating the nonbonding interaction energy to the template ability to form a porous structure is proposed as a step toward a better understanding of the role of the organic template in the synthesis of porous molecular sieves.

Keywords: $AlPO_4$-5; Molecular sieves; Synthesis; Organic template; DFT; XRD

1. Introduction

In the synthesis of phosphate- or silicate-based microporous molecular sieves (MMS), organic amines or quaternary ammonium ions are usually used as templates or structure directing agents. It is believed that these organic templates stabilize certain phases during the synthesis course via nonbonding interactions between the template and the host inorganic framework [1]. Actually, the role of the organic template still remains an important issue that is not yet clearly understood in the synthesis of MMS [2–4]. Obviously, understanding this role will be crucial for the rational design of MMS. An early computational study on different types of templates and several zeolite structures showed, although not in all cases, a fair correlation between the nonbonding energy values and the experimentally used templates [5]. The packing effect of the occluded templates was also considered to explain the structure directing role of several organic templates [5,6]. These findings led to the development of de novo methodologies to help predicting the most successful template for a given framework [7]. As a result of the extensive research in this area, a widely used empirical view stating that "a successful template has a good fit with the host framework" was sealed. However, this empirical view could not explain the following experimental observations. The first one is "one-template/multiple-structures" as in the case of di-*n*-propylamine that is used in the synthesis of more than 10 different AlPO structures, such as $AlPO_4$-11, $AlPO_4$-31, $AlPO_4$-39, $AlPO_4$-41, $AlPO_4$-43, $AlPO_4$-46, $AlPO_4$-47, and $AlPO_4$-50 [8]. The second one is "multiple-templates/one-structure" as in the case of $AlPO_4$-5 which could be prepared using more than 25 different templates [2,8]. It should be mentioned here that methyldicyclohexylamine [9], 8-hydroxyquinoline [10], benzyl-pyrrolidine and its fluorinated derivatives [11], and tetrabutylammonium hydroxide (TBAOH) [12] are the most recently used templates for $AlPO_4$-5 synthesis. This difficulty of understanding the role of organic templates arises from the complexity of the hydrothermal crystallizations, the lack of information on the presence of different chemical species at different synthesis stages, and the lack of complete understanding of the principles governing the formation of crystalline porous materials [13]. Therefore, enhanced efforts and new ideas are needed for a better understanding of the role of the organic templates in the synthesis of MMS.

* Corresponding author. Tel.: +32 81724531; fax: +32 81725414.
** Corresponding author. Tel.: +32 81724534; fax: +32 81725466.
E-mail addresses: bao-lian.su@fundp.ac.be (B.-L. Su), daniel.vercauteren@fundp.ac.be (D.P. Vercauteren).

1381-1169/$ – see front matter © 2007 Elsevier B.V. All rights reserved.
doi:10.1016/j.molcata.2007.02.015

The $AlPO_4$-5 structure attracted a considerable attention in materials science [14] and catalysis [15,16] applications, on one hand due to its large pores (pore diameter 7.3 Å [17], which can accommodate relatively large molecules [18,19]) and on the other hand to the ease of its synthesis.

In this study, we monitor the hydrothermal genesis of the $AlPO_4$-5 structure in the crystallization temperature range 130–150 °C using four different organic templates, viz., methyldicyclohexylamine (MCHA), triethylamine (TEA), tripropylamine (TPA), and tetraethylammonium hydroxide (TEAOH), by X-ray powder diffraction (XRD). Moreover, periodic density functional theory (DFT) calculations were employed to investigate the template–framework interactions.

2. Experimental synthesis, models, and computational details

2.1. Experimental synthesis

The synthesis gels of molar compositions Al_2O_3:P_2O_5:R (R = MCHA, TEA, TPA, or TEAOH):250H_2O were prepared by first adding pseudoboehmite (Dequagel HP300, Dequachim) to a diluted phosphoric acid 85% (Aldrich). After 1 h of stirring, corresponding amounts of organic amine templates were added dropwise. The gels were stirred further for 1 h more before transferring into Teflon-lined stainless steel autoclaves. The reaction mixtures were heated at the desired temperatures under autogenous pressure for 20 h. The white powders, obtained after decantation and filtration, were dried at 110 °C for 3 h.

The as-synthesized materials were investigated by XRD in the range 5–40° of 2θ with step size 0.02°. A copper anticathode producing X-rays with a wavelength equal to 1.54178 Å (Philips PW 170) was used.

2.2. Models and computational details

$AlPO_4$-5 (IZA code AFI) has a hexagonal structure with one-dimensional channels of nearly spherical pores (pore diameter 7.3 Å [17]). These channels are composed by 12-membered rings running along the *c*-direction. The whole unit cell of $AlPO_4$-5 containing 72 ions is considered by applying periodic boundary conditions.

Geometry optimizations and energy calculations were carried out using density functional theory (DFT) employing the DMol^3 software in the MS Modelling 4.0 package [20–22], at the generalized gradient approximation (GGA) level with the Hamprecht, Cohen, Tozer, and Handy (HCTH) exchange and correlation functional [23–25]. It has been shown that the HCTH functional has a greater universality than the previous GGA functionals and that it performs well for systems prevailing weak interactions [26]. Double numerical basis set with single polarization functions (DNP) on a medium quality integration grid (program default) was used in all calculations. Moreover, the DNP basis set produces small basis set superposition errors [27,28]. The nonbonding interaction energy E_{Inter} was calculated as:

$$E_{Inter} = E_{AlPO_4\text{-}5/TM} - E_{AlPO_4\text{-}5} - E_{TM}$$

where $E_{AlPO_4\text{-}5/TM}$, $E_{AlPO_4\text{-}5}$, and E_{TM} refer to the calculated total energy of the system, i.e., template inside $AlPO_4$-5, $AlPO_4$-5, and organic amine template, respectively. It should be mentioned here that the main interest is to measure the nonbonding interactions in a relative way rather than looking for absolute values.

Molecular mechanics (Hyperchem 7.5 code [29]) and simulated annealing (AMPAC 8.16 code [30]) type calculations were performed first to get the most stable conformations of the organic amine templates, which were further optimized geometrically by DFT. In the case of a protonated organic template, an OH^- group was added as a counter ion to avoid the infinite electrostatic repulsions between charged unit cells upon applying periodic boundary conditions. However, an unfavorable abstraction of one of the hydrogen atoms in the protonated template by OH^- was observed. Here, water molecules are necessary to stabilize the organic cation and the counter ion. We found that three water molecules located mostly between the OH^- and the organic cations are quite sufficient for this purpose. The protonated templates, OH^-, and water molecules were fully optimized together prior to their introduction in the channels of $AlPO_4$-5. For the occluded organic templates, considered neutral or protonated, we tried manually several initial orientations for each template until the most stable interaction with the framework was obtained.

3. Results and discussion

Fig. 1a–d shows the XRD patterns of the as-synthesized solids obtained at different crystallization temperatures (130–150 °C). At 130 °C (Fig. 1a), only the TEAOH template could form the $AlPO_4$-5 phase. This is indicated by the weak reflection at 2θ = 7.32°, which is characteristic of the (1 0 0) crystallographic plane of $AlPO_4$-5 [31,32]. Other templates, i.e., MCHA, TEA, and TPA form the $AlPO_4$-C phase [31] (IZA code APC [17]) with different degrees of crystallinity. The appearance of $AlPO_4$-C was previously observed during the synthesis of $AlPO_4$-5 with *ortho*-fluorobenzyl-pyrrolidine [11]. At higher crystallization temperature, i.e., 140 °C (Fig. 1b), stronger reflections due to $AlPO_4$-5 could be observed with TEAOH. With MCHA and TPA, there are no clear reflections due to $AlPO_4$-5. This suggests the inability of these templates to form $AlPO_4$-5 at least under such experimental condition. Performing the synthesis at higher crystallization temperature, i.e., 145 °C, reflections due to $AlPO_4$-5 can be observed using TEA or MCHA along with the $AlPO_4$-C phase. Here again TEAOH gives the strongest $AlPO_4$-5 reflections for $AlPO_4$-5. By increasing the crystallization temperature up to 150 °C, the XRD reflections due to $AlPO_4$-5 become clearer in the case of TEA and MCHA. Moreover, TEAOH templated $AlPO_4$-5 gives strong reflections. Under this condition, TPA templated $AlPO_4$-5 starts giving weak reflection at 2θ = 7.50°. Thus, it is clear from Fig. 1a–d that TEAOH has the best ability or templating power to form $AlPO_4$-5 as compared to the other investigated templates. Interestingly, it can be seen that the ability of the organic template to direct the synthesis gel toward $AlPO_4$-5 formation is enhanced by increasing the crystallization

temperature in such a way that at 170 °C with gel composition (Al_2O_3:P_2O_5:R:100H_2O), all templates could generate the formation of well-crystalline $AlPO_4$-5 structures as shown in Fig. 1e. Therefore, investigating the hydrothermal genesis of $AlPO_4$-5 is more appropriate for studying the templating effect rather than the general ability of a template to synthesize $AlPO_4$-5, which is strongly dependent on the experimental synthesis conditions.

To evaluate if the above suggested results present new concepts in the formation of MMS or it was accidentally obtained, we also performed the synthesis under different experimental conditions, such as: (i) addition of 0.5 M HF to the synthesis gels, (ii) using microwave (MW) irradiation in $AlPO_4$-5 synthesis, and (iii) carrying out the synthesis from more concentrated gels. Fig. 2a–f presents the XRD patterns for the as-synthesized samples prepared under these different experimental conditions.

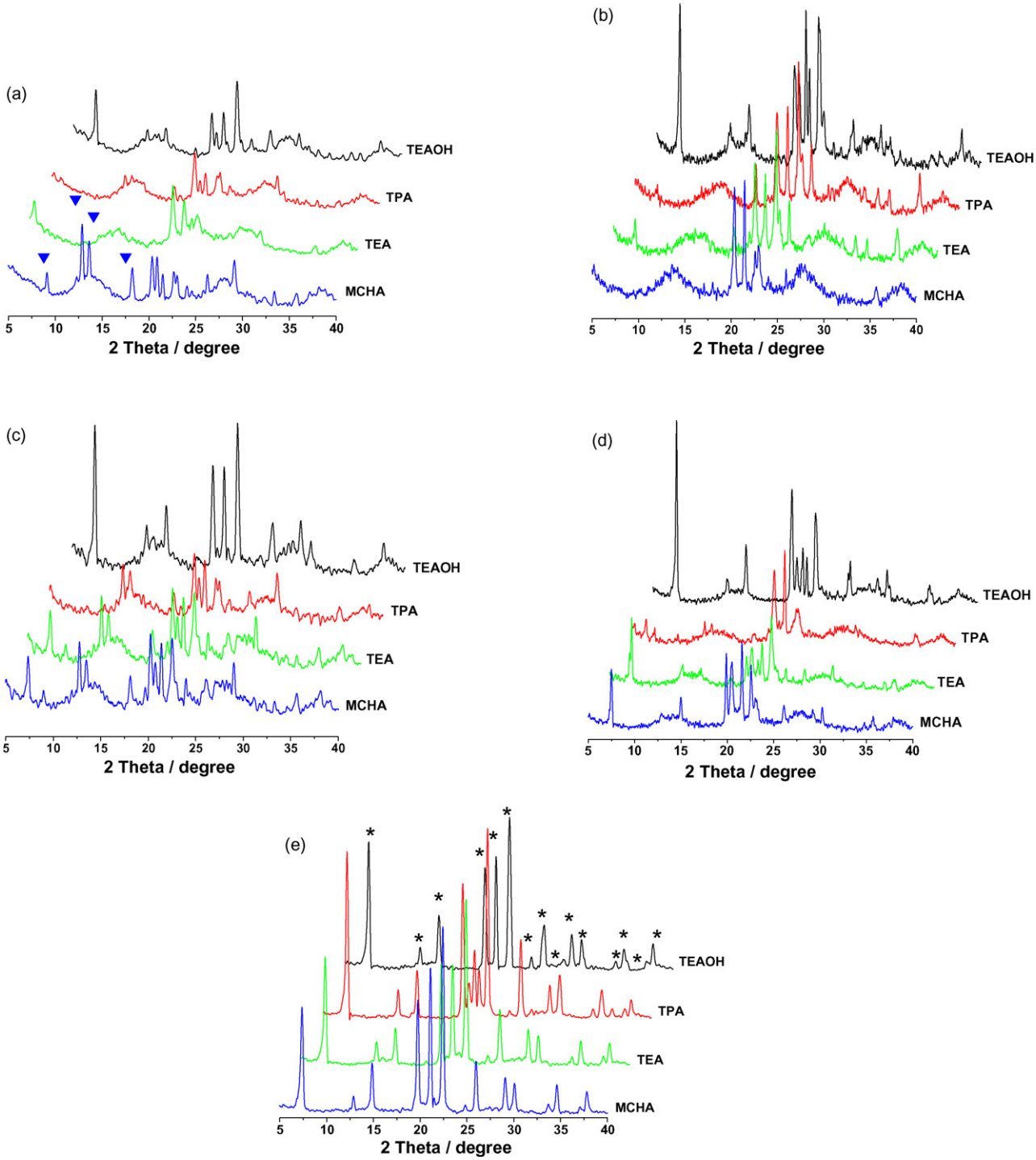

Fig. 1. XRD patterns of the as-synthesized solid products at different crystallization temperatures for 20 h: (a) 130 °C, (b) 140 °C, (c) 145 °C, (d) 150 °C, and (e) Al_2O_3:P_2O_5:R:100H_2O at 170 °C. Reflections due to $AlPO_4$-5 and $AlPO_4$-C are marked by (*) and (▼), respectively.

In more details, Fig. 2a and b shows the XRD patterns after addition of 0.5 M HF to the synthesis gels prepared at 130 and 140 °C, respectively. At 130 °C, very weak reflections indicate the presence of small amount of the $AlPO_4$-5 phase in the case of TEAOH. However, in the case of the other templates no $AlPO_4$-5 reflections could be observed. The same behavior is noticed at higher crystallization temperature, i.e., 140 °C as shown in Fig. 2b, except that TEAOH templated products produces stronger reflections at higher crystallization temperature. It is important to compare the XRD patterns presented in Fig. 2a and b, i.e., after HF addition, with those without HF illustrated in Fig. 1a and b. It can be seen that HF addition delays

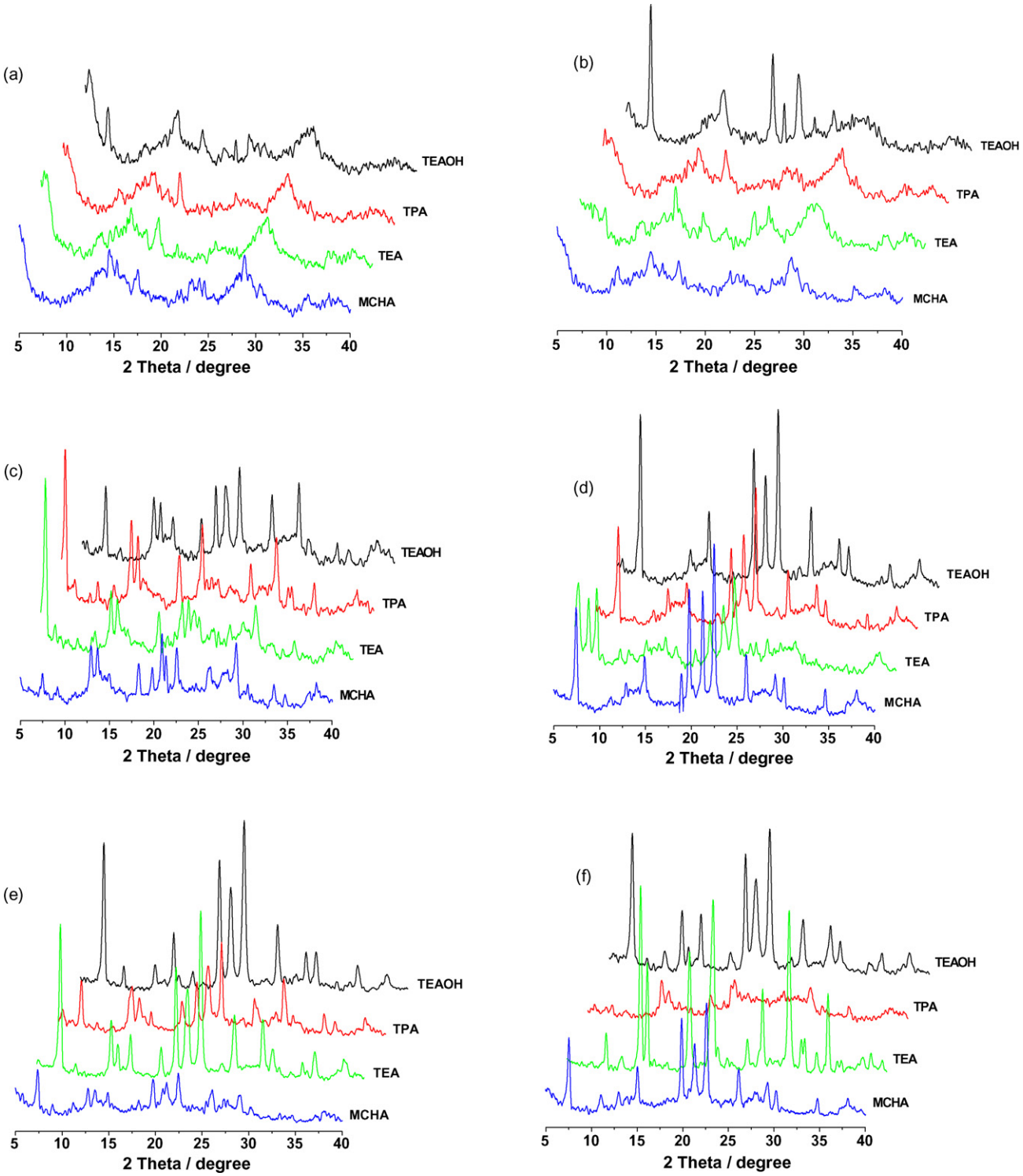

Fig. 2. XRD patterns of the as-synthesized solid products used to monitor the genesis of $AlPO_4$-5 under different synthesis conditions: (a) 130 °C with HF, (b) 140 °C with HF, (c) microwave at 130 °C, (d) microwave at 140 °C, (e) concentrated gel at 130 °C, and (f) concentrated gel at 126 °C.

the crystallization of $AlPO_4$-5 due to its mineralizing effect [3,4].

Fig. 2c and d shows the XRD patterns of the as-synthesized samples produced under microwave irradiation (MW) for 45 min at 130 and 140 °C, respectively. It can be seen that only TEAOH could give XRD reflections due to $AlPO_4$-5 at 130 °C. However, at 140 °C all templates could form $AlPO_4$-5 crystals. It is interesting to note that the intermediates during the MW synthesis are different from those observed earlier under hydrothermal heating. It is thus valuable to devote a separate detailed study to follow the possible intermediates formed during the synthesis of $AlPO_4$-5 by different organic templates at 130 and 140 °C, respectively. Finally, we monitored the genesis of $AlPO_4$-5 from more concentrated gels (i.e., Al_2O_3:P_2O_5:R:55H_2O) at 130 and 126 °C as shown in Fig. 2e and f, respectively. It is important to mention here that all templates could form $AlPO_4$-5 at 130 °C. The strongest reflections are found with TEAOH and TEA. By comparing the results in Fig. 2e with the XRD results in Figs. 1a and 2a or b, one can conclude that the crystallization of $AlPO_4$-5 from concentrated gels will be better. This fact was used already to obtain good $AlPO_4$-5 crystals with minimal solvent wast [33]. In order to differentiate between the templates on the basis of their templating power, we have lowered the crystallization temperature to 126 °C as presented in Fig. 2f. It can be seen that the strongest XRD reflections are observed with TEAOH. MCHA could also form $AlPO_4$-5. However, TEA forms $AlPO_4$-C first and TPA gives very weak reflections for $AlPO_4$-C. The formation of $AlPO_4$-C at low crystallization temperature can be attributed to the worse template ability to direct the synthesis toward the open framework $AlPO_4$-5 structure [11]. Apparently, templates MCHA, TEA, and TPA, are preferable than TEAOH in directing the synthesis to the $AlPO_4$-C structure. A separate detailed study would be, however, necessary to confirm this trend.

Table 1 presents several of the optimized parameters calculated for the organic templates used in the synthesis of $AlPO_4$-5. Since the genesis of AlPOs are carried out under acidic condition, the organic amine templates are mostly protonated [34]. Therefore, protonated forms of MCHA, TEA, and TPA are also considered. In the case of neutral amines, the C–N bond distances are in very good agreement with the reported value for C–N_{sp3} (1.468 Å) [35]. By comparing the C–N distances and Mulliken charges of the H and N atoms in neutral and protonated templates, one can see that protonation of neutral amine leads to an increase of the C–N distance, a decrease of the negative charge on N and an increase of the positive charge on H. Thus, a stronger nonbonding interaction energy between the template and the $AlPO_4$-5 framework is expected in the case of protonated amines. The increase of the calculated C–N distances in protonated templates, as compared to neutral ones, is also in agreement with the reported values for $(C)_3$–NH^+,1.502 Å and for $(C)_4$–NH^+, 1.509 Å [35]. This reported trend is reflected here by the slight increase in C–N distance, 1.526 Å, of TEAOH as compared to C–N of protonated TEA, 1.518 Å, and of protonated TPA, 1.515 Å. The calculated C–N distance of protonated MCHA is an exception to this trend. This can be attributed to the steric hindrance excerted by the two cyclohexyl rings.

Fig. 3a–d shows the optimized structures of $AlPO_4$-5 frameworks (super cells 2 × 2 × 2) occluding MCHA, TEA, TPA, and TEAOH, respectively. The calculated nonbonding interaction energy values are given in Table 1 and Fig. 3e. It should be remined here that for all protonated template models as in the case of TEAOH shown in Fig. 3d, we considered an OH^- counter ion and water molecules to mimic the synthesis conditions and to make our models more realistic.

DFT calculation results for the nonbonding interaction energy given in Table 1 and described by Fig. 3e can be summarized in the following points: (i) TEAOH has the strongest nonbonding interactions, i.e., the lowest E_{Inter} value (−261.2 kJ/mol) when compared with the other protonated templates, i.e., protonated MCHA, −147.6 kJ/mol, protonated TEA, −189.3 kJ/mol, and protonated TPA, −133.4 kJ/mol. (ii) Neutral templates induce weaker interactions as compared to their protonated forms. This trend was shown previously for neutral and charged templates by Lewis [36]. Therefore, one can conclude that the best ability of TEAOH observed earlier in the genesis of $AlPO_4$-5, under the different synthesis conditions considered here, is attributed to the stronger nonbonding interaction energy between the framework and the TEAOH template. The appreciable E_{Inter} values calculated for protonated TEA and MCHA could explain their better ability to form $AlPO_4$-5 as compared to protonated TPA. These observations ensure the applicability of the proposed new approach correlating the calculated nonbonding interaction energy to the template ability to form $AlPO_4$-5. It should be mentioned that although it is not known clearly yet which step is the most important one to be modeled in the hydrothermal synthesis of MMS, i.e., oligomerization of aluminophosphate intermediates, nucleation or crystal growth,

Table 1
Several optimized parameters and total energies of the various organic amine templates

	MCHA	TEA	TPA	TEAOH
C–N	1.462 (1.535)[a]	1.462 (1.518)	1.460 (1.515)	1.526
qN	−0.085 (−0.047)	−0.100 (−0.039)	−0.098 (−0.039)	−0.055
qH	0.120 (0.158)	0.114 (0.163)	0.111 (0.142)	0.179
E_{TM}	−565.3327 (−871.1551)	−292.5036 (−598.3416)	−410.4830 (−716.3221)	−676.9718
$E_{AlPO_4-5/TM}$	−11187.6940 (−11493.5584)	−10914.8758 (−11220.7608)	−11032.8480 (−11338.7201)	−11299.4184
E_{Inter}[b]	−37.3 (−147.6)	−65.9 (−189.3)	−46.9 (−133.4)	−261.2

Bond distances are given in (Å), Mulliken charges in (e^-), and energy values in (au). $E_{AlPO_4-5} = -10622.3471$ au.

[a] Values for protonated amines are given between parentheses.

[b] E_{Inter} (kJ/mol).

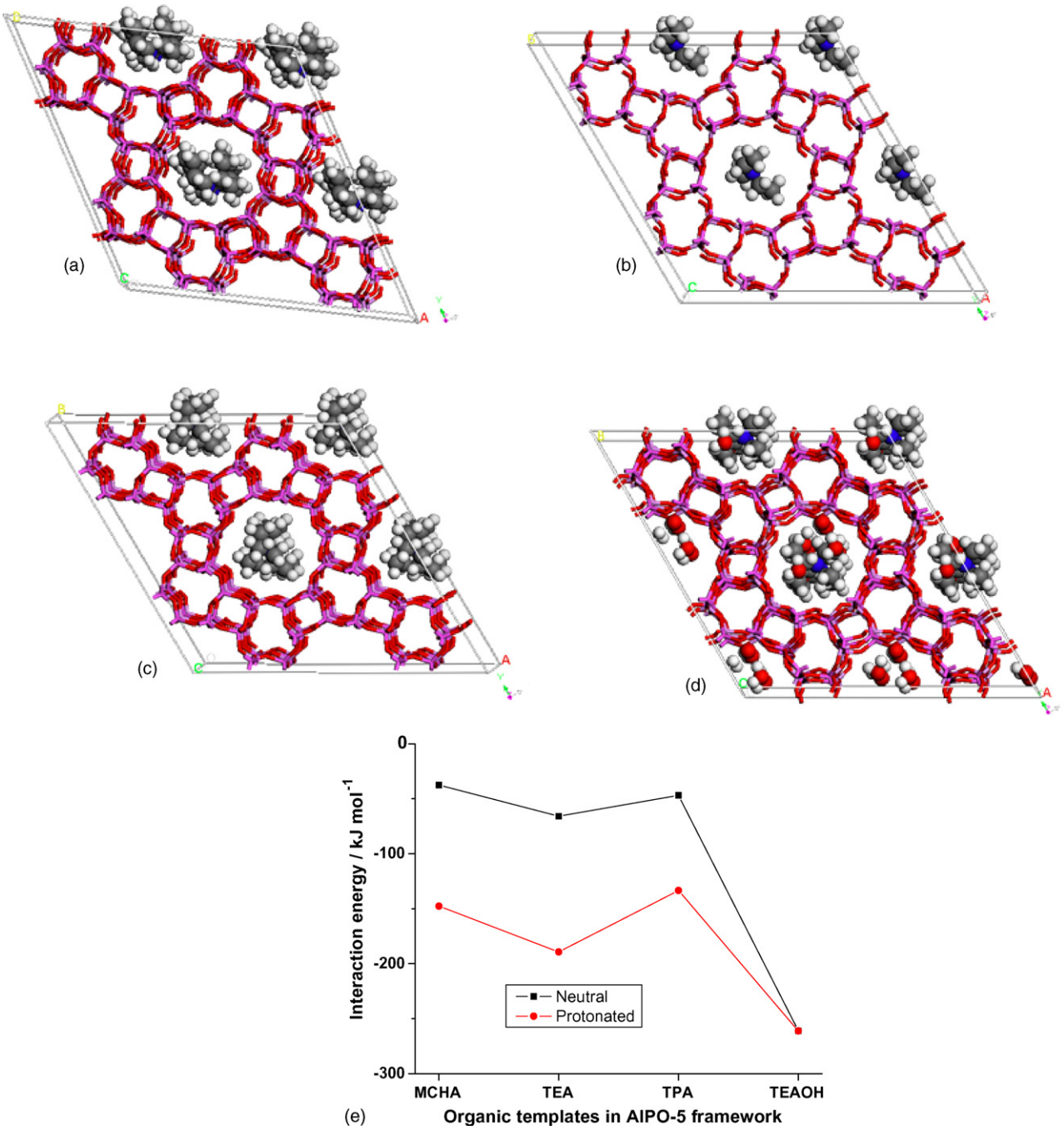

Fig. 3. Optimized structures of $AlPO_4$-5 (super cells $2 \times 2 \times 2$) occluding the different organic templates used in the synthesis: (a) $AlPO_4$-5/MCHA, (b) $AlPO_4$-5/TEA, (c) $AlPO_4$-5/TPA, (d) $AlPO_4$-5/TEAOH-H_2O, and (e) calculated nonbonding interaction energy between the templates and $AlPO_4$-5 frameworks.

it has been claimed that computational studies starting with the MMS model could give useful information about templating effect, template selection, and template prediction [5,7,36].

4. Conclusions

The genesis of $AlPO_4$-5 crystals has been monitored by XRD in the presence of different organic templates, viz., MCHA, TEA, TPA, and TEAOH under different synthesis conditions. Results show that the TEAOH template has the best ability to form the $AlPO_4$-5 structure from the synthesis gel. This high templating power of TEAOH was not affected by changing the synthesis conditions. Density functional theory (DFT) calculations, on periodic models of $AlPO_4$-5, indicate the stronger nonbonding interaction energy in the case of protonated templates as compared to neutral ones. Furthermore, the strongest nonbonding interaction energy was found between TEAOH and the $AlPO_4$-5 framework.

Finally, we propose a new approach, correlating the calculated nonbonding interaction energy and the template ability to form a given $AlPO_4$-5 in particular. The proposed approach also can be applied in general to the synthesis of templated

microporous molecular sieves. We believe that this view gives a better understanding of the role of organic templates in the synthesis of porous molecular sieves.

Acknowledgements

M.E. thanks the Interuniversity research program (PAI/IUAP05/01) on "Quantum size effects in nanostructured materials" for a post-doctoral fellowship. The authors acknowledge gratefully performing all calculations on the Interuniversity Scientific Computing Facilities (ISCF), installed at FUNDP, and the financial support of the FNRS-FRFC, and the Loterie Nationale for the convention no. 2.4578.02.

References

[1] L. Gómez-Hortigüela, J. Pérez-Pariente, F. Corà, C.R.A. Catlow, T. Blasco, J. Phys. Chem. B 109 (2005) 21539.
[2] B.M. Lok, T.R. Cannan, C.A. Messina, Zeolites 3 (1983) 282.
[3] C.S. Cundy, P.A. Cox, Microporous Mesoporous Mater. 82 (2005) 1.
[4] N. Rajić, J. Serb. Chem. Soc. 70 (2005) 371.
[5] D.W. Lewis, C.M. Freeman, C.R.A. Catlow, J. Phys. Chem. 99 (1995) 11194.
[6] L. Gómez-Hortigüela, F. Corà, C.R.A. Catlow, J. Pérez-Pariente, J. Am. Chem. Soc. 126 (2004) 12097.
[7] D.W. Lewis, D.J. Willock, C.R.A. Catlow, J.M. Thomas, G.J. Hutchings, Nature 382 (1996) 604.
[8] J. Yu, R. Xu, Chem. Soc. Rev. 35 (2006) 593.
[9] M. Sanchez-Sanchez, G. Sankar, A. Simperler, R.G. Bell, C.R.A. Catlow, J.M. Thomas, Catal. Lett. 88 (2003) 163.
[10] H. Li, G. Zhu, X. Guo, Y. Li, C. Li, S. Qiu, Microporous Mesoporous Mater. 85 (2005) 324.
[11] L. Gómez-Hortigüela, J. Pérez-Pariente, T. Blasco, Microporous Mesoporous Mater. 78 (2005) 189.
[12] F.Y. Jiang, Z.K. Tang, J.P. Zhai, J.T. Ye, J.R. Han, Microporous Mesoporous Mater. 92 (2006) 129.
[13] C.S. Cundy, P.A. Cox, Chem. Rev. 103 (2003) 663.
[14] G. Schulz-Ekloff, D. Wöhrle, B. van Duffel, R.A. Schoonheydt, Microporous Mesoporous Mater. 51 (2002) 91, and references therein.
[15] H. Maekawa, S.K. Saha, S.A.R. Mulla, S.B. Waghmode, K. Komura, Y. Kubota, Y. Sugi, J. Mol. Catal. A 263 (2007) 238.
[16] W. Fan, B. Fan, M. Song, T. Chen, R. Li, T. Dou, T. Tatsumi, B.M. Weckhuysen, Microporous Mesoporous Mater. 94 (2006) 348.
[17] W.M. Meier, D.H. Olson, Ch. Baerlocher, Atlas of Zeolite Framework Types, fifth rev. ed., Elsevier, London, 2001.
[18] G. Ihlein, F. Schüth, O. Krauβ, U. Vietze, F. Laeri, Adv. Mater. 10 (1998) 1117.
[19] M. Ganschow, C. Hellriegel, E. Kneuper, M. Wark, C. Thiel, G. Schulz-Ekloff, C. Bräuchle, D. Wöhrle, Adv. Funct. Mater. 14 (2004) 269.
[20] B. Delley, J. Chem. Phys. 92 (1990) 508.
[21] B. Delley, J. Chem. Phys. 113 (2000) 7756.
[22] www. Accelrys.com/.
[23] F.A. Hamprecht, A.J. Cohen, D.J. Tozer, N.C. Handy, J. Chem. Phys. 109 (1998) 6264.
[24] A.D. Boese, N.L. Doltsinis, N.C. Handy, M. Sprik, J. Chem. Phys. 112 (2000) 1670.
[25] A.D. Boese, N.C. Handy, J. Chem. Phys. 114 (2001) 5497.
[26] D. Kim, T.B. Lee, S.B. Choi, J.H. Yoon, J. Kim, S.-H. Choi, Chem. Phys. Lett. 420 (2006) 256.
[27] J. Sauer, in: C.R.A. Catlow (Ed.), Modelling of Structure and Reactivity in Zeolites, Academic Press, London, 1992, pp. 206–207.
[28] N. Govind, J. Andzelm, K. Reindel, G. Fitzgerald, Int. J. Mol. Sci. 3 (2002) 423.
[29] Hypercube Inc. HyperChem Professional Release 7.5 for Windows, 2003.
[30] D.A. Liotard, G.D. Hawkins, D.M. Dolney, D. Rinaldi, C.J. Cramer, D.G. Truhlar, AMPAC-8.16, Semichem, Shawnee, USA, 2005.
[31] M.M.J. Treacy, J.B. Higgins, Collection of Simulated XRD Powder Patterns for Zeolites, fourth rev. ed., Elsevier, London, 2001.
[32] S.H. Jhung, J.-S. Chang, Y.K. Hwang, S.-E. Park, J. Mater. Chem. 14 (2004) 280.
[33] Y. Wan, C.D. Williams, J.J. Cox, C.V.A. Duke, Green Chem. 1 (1999) 169.
[34] S. Ashtekar, P.J. Barrie, M. Hargreaves, L.F. Gladden, Angew. Chem. Int. Ed. Engl. 36 (1997) 876.
[35] D.R. Lide, Handbook of Chemistry and Physics, 84th ed., CRC press, Washington DC, 2004, pp. 5–9.
[36] D.W. Lewis, in: C.R.A. Catlow, R.A. van Santen, B. Smit (Eds.), Computer Modelling of Microporous Materials, Elsevier Ltd., London, 2004, p. 243.